Author's Accepted Manuscript

Low-fired fluoride microwave dielectric ceramics with low dielectric loss

Xiao-Qiang Song, Kang Du, Jie Li, Xue-Kai Lan, Wen-Zhong Lu, Xiao-Hong Wang, Wen Lei

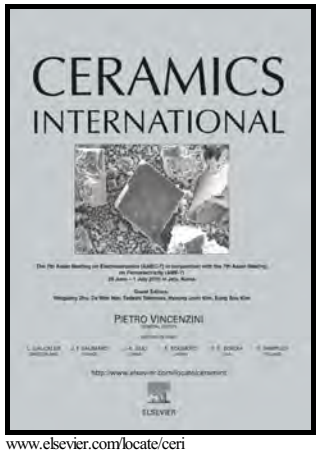

www.elsevier.com/locate/ceri

PII: S0272-8842(18)32627-0
DOI: https://doi.org/10.1016/j.ceramint.2018.09.164
Reference: CERI19563

To appear in: *Ceramics International*

Received date: 17 August 2018
Revised date: 8 September 2018
Accepted date: 16 September 2018

Cite this article as: Xiao-Qiang Song, Kang Du, Jie Li, Xue-Kai Lan, Wen-Zhong Lu, Xiao-Hong Wang and Wen Lei, Low-fired fluoride microwave dielectric ceramics with low dielectric loss, *Ceramics International,* https://doi.org/10.1016/j.ceramint.2018.09.164

This is a PDF file of an unedited manuscript that has been accepted for publication. As a service to our customers we are providing this early version of the manuscript. The manuscript will undergo copyediting, typesetting, and review of the resulting galley proof before it is published in its final citable form. Please note that during the production process errors may be discovered which could affect the content, and all legal disclaimers that apply to the journal pertain.

ACCEPTED MANUSCRIPT

Low-fired fluoride microwave dielectric ceramics with low dielectric loss

Xiao-Qiang Song[a,b], Kang Du[a,b], Jie Li[a,b], Xue-Kai Lan[a,b], Wen-Zhong Lu[a,b], Xiao-Hong Wang[a,b], Wen Lei[a,b*]

[a] School of Optical and Electronic Information, Huazhong University of Science and Technology, Wuhan 430074, P. R. China

[b] Key Lab of Functional Materials for Electronic Information (B), Ministry of Education, Wuhan 430074, P. R. China

*Corresponding author. Tel.: +86 27 8755 6493; fax: +86 27 8754 3134. *E-mail address:* wenlei@mail.hust.edu.cn (W. Lei)

Accepted manuscript

Abstract

Low-fired fluoride microwave dielectric ceramics (LiF, CaF_2, SrF_2 and BaF_2) were prepared through a simple one-step sintering process. Fluoride ceramics, especially LiF, which had the lowest sintering temperature of 800 °C, could be well sintered below 1050 °C. Rietveld refinement results showed that LiF, CaF_2, SrF_2 and BaF_2 ceramics crystallized into a cubic structure with space group Fm-3m. The relative permittivity (ε_r), quality factor ($Q\times f$) and temperature coefficient of the resonant frequency (τ_f) of the fluoride ceramics were closely related to relative density, the ionic polarizability of the primitive unit cell, the packing fraction and the bond valence. In this series of low-permittivity fluoride ceramics, LiF, CaF_2 and BaF_2 could be co-fired with Ag powders, and LiF ceramic exhibited the highest $Q\times f$ value of

ACCEPTED MANUSCRIPT

73880 GHz, which is comparable to those of traditional oxide microwave dielectric ceramics.

1. Introduction

Low-temperature co-fired ceramics (LTCC) technology is a potential technology for satisfying the miniaturization and multifunction requirements of electronic devices. For practical applications, LTCC must have a low relative permittivity ($\varepsilon_r < 15$) to reduce the signal propagation delay time, a high quality factor ($Q \times f$) for frequency selectivity, and a near zero temperature coefficient of resonant frequency ($-10 \leq \tau_f \leq +10$ ppm/°C) to ensure the stability of devices with temperature fluctuations [1,2]. Furthermore, these materials should be sintered below 961 °C to be co-fired with Ag electrode [3]. Unfortunately, the sintering temperatures of most microwave dielectric ceramics are too high to be co-fired with Ag electrode. Previous studies have used many types of glass frits and low-melting-point oxides to decrease the sintering temperature of microwave dielectric ceramics [4,5]. The $Q \times f$ value is seriously deteriorated because of the high dielectric loss of the glass phase.

Some microwave dielectric ceramics with low sintering temperature have been explored, such as $Li_2ZnGe_3O_8$, Li_4WO_5 and Bi_3NbO_7, to meet both dielectric properties and sintering temperature requirements [2,6,7]. However, most high-performance microwave dielectric ceramics, such as $ZnAl_2O_4$, Mg_2SiO_4 and $Mg_4Nb_2O_9$ [8-10], still cannot be used as LTCC because of their high sintering temperature.

Aside from glass frits and low-melting-point oxides, fluorides are also a large type of sintering aids. LiF has a melting point of approximately 845 °C, whereas CaF_2, SrF_2 and BaF_2 have a melting point of approximately 1400 °C [11]. Table 1 presents the sintering temperatures and microwave dielectric properties of some microwave dielectric ceramics doped with different fluorides. The $Q\times f$ values of the samples listed in Table 1 have not deteriorated apparently, which means that fluorides have more advantages than glass frits as sintering aids. The sintering temperatures of fluoride-doped samples are much lower than those of pure phases. The $BaAl_2Si_2O_8$-LiF and $MgTiO_3$-CaF_2 systems can be sintered at 900 °C and 1050 °C [12,19], which indicates that pure LiF and CaF_2 may be sintered below 900 °C and 1050 °C.

LiF and AF_2 (A = Ca, Sr, Ba) have typical rock-salt and fluorite-type structures, respectively. Many compounds with rock-salt or fluorite-type structure have good microwave dielectric properties, such as Li_4WO_5, $Li_2Mg_3TiO_6$ and CeO_2 [6,20,21]. From the perspective of the relationship between crystal structure and microwave dielectric properties, LiF and AF_2 (A = Ca, Sr, Ba) ceramics may also have good microwave dielectric properties. In 2004, Geyer et al. [22] reported the microwave dielectric properties of LiF, CaF_2, SrF_2, BaF_2 and MgF_2 single crystals, and their $Q\times f$ values are 192400, 92000, 73000, 57600 and 458600 GHz, respectively. Zhang et al. [16] designed a new type of fluorine-containing ceramic $Li_{2+x}Mg_{1-x}Ti_3O_{8-x}F_x$, which shows good microwave dielectric properties with ε_r = 24.8, $Q\times f$ = 50000 GHz and τ_f =

-6.09 ppm/°C. Previous studies reported that some fluorides and fluorine-containing ceramics should also have good microwave dielectric properties, indicating that the research field of microwave dielectric ceramics may be expanded from oxides to fluorides.

In this study, LiF, CaF_2, SrF_2 and BaF_2 ceramics were prepared through a simple one-step sintering process. The sintering behavior, microstructure, and the relationship between the crystal structure and microwave dielectric properties of fluoride ceramics were investigated.

2. Experimental procedure

LiF, CaF_2, SrF_2 and BaF_2 ceramics were prepared through a one-step sintering process using reagent grade LiF (99.5%), CaF_2 (98.5%), SrF_2 (99.0%), BaF_2 (99.0%) and Ag (99.99%) powders as raw materials. Unlike the traditional solid state reaction method, the raw materials need not be ball milled and calcined. The powders were uniaxially pressed into samples directly under a pressure of 150 MPa without the granulate processing with PVA binder. The samples were 12 mm in diameter and 6 mm in height. They were sintered in the temperature range of 675 °C-1075 °C for 3 h at a heating rate of 5 °C/min in air.

The bulk density of the sintered samples was measured by Archimedes method. The relative density ρ_{rel} was obtained by:

$$\rho_{rel} = \frac{\rho_{bul}}{\rho_{the}} \qquad (1)$$

where ρ_{bul} and ρ_{the} are the bulk density and theoretical densities, respectively.

ACCEPTED MANUSCRIPT

The XRD data were obtained using X-ray diffraction (XRD-7000, Shimadzu, Kyoto, Japan) with CuKα radiation. Phase analysis was performed by Rietveld refinement using GSAS and EXPGUI software [23-25]. The microstructure was observed by scanning electron microscopy (SEM, Sirion 200, Netherlands). The ε_r and the unloaded $Q\times f$ value were measured at 12-15 GHz in the TE_{011} mode by Hakki and Coleman method [26] using a network analyzer (Agilent E8362B, Agilent Technologies, USA) and parallel silver boards. The τ_f value in the temperature range of 30 °C to 80 °C was calculated by the following formula:

$$\tau_f = \frac{1}{f(T_0)} \frac{[f(T_1) - f(T_0)]}{T_1 - T_0} \quad (2)$$

where $f(T_1)$ and $f(T_0)$ represent the resonant frequency at T_1 (80 °C) and T_0 (30 °C), respectively.

3. Results and discussion

Fig. 1 shows the X-ray diffraction (XRD) patterns of fluoride raw materials and sintered ceramics for preparation at different densification temperatures. The diffraction peaks corresponding to the LiF, CaF_2, SrF_2 and BaF_2 raw materials (Fig. 1(a)–(d)) and sintered ceramics (Fig. 1(e)–(h)) are indexed by cubic LiF (PDF#45-1460), CaF_2 (PDF#65-0535), SrF_2 (PDF#88-2294) and BaF_2 (PDF#85-1342), respectively. Fig. 2 and Table 2 show the results of Rietveld refinement for fluoride ceramics that belong to the Fm-3m (225) space group.

Accepted manuscript

ACCEPTED MANUSCRIPT

Fig. 3(a)-(d) shows the scanning electron micrographs of the fluoride ceramics sintered at their optimum sintering temperature. The surface of the fluoride ceramics has some pores, indicating that the ceramics have low relative densities (Table 2). The grain size of LiF ceramic is much larger than those of the other fluoride ceramics, but its pores are also significant. For CaF_2, SrF_2 and BaF_2 ceramics, the distribution of grain size is highly inhomogeneous, but they have fewer pores than LiF ceramic. The microstructure of this series of fluoride ceramics are extremely different from those of cubic oxide ceramics.

In general, the (100) crystal face has low surface free energy, whereas the (111) crystal face has high surface free energy [27]. Thus, the growth speed in the [111] direction is faster than that in the [100] direction, which is similar to that in the cubic perovskite structure. Finally, the shape of the grain is an ideal cube for this series of fluoride ceramics (Fig. 3(e)). However, the sintering theory for fluoride is different from that of oxide ceramics. Bullard et al. [28] investigated the microstructure development during lithium fluoride sintering. Their findings, which are consistent with ours, showed that LiF is more diffcult to densify than other oxide ceramics. The main mass transport mechanism for LiF is vapor transport, and surface diffusion and grain boundary migration are minor contributors to coarsening. The (100) surface free energy of LiF is 340 erg/cm^2, which is relatively lower than the 905 and 1000 erg/cm^2 of Al_2O_3 and MgO, respectively. Low surface free energy leads to a low driving force for the densification of LiF. Given the substantial surface diffusion, the breakup of pore channels into isolated voids begins early. The pressure of trapped air in the

ACCEPTED MANUSCRIPT

isolated pores reduces the driving force for densification. Therefore, the low driving force for densification and gas entrapment are the main causes of low density. These porous microstructures negatively effect on microwave dielectric properties, which will be discussed later.

Fig. 4 shows the variations in the relative densities and microwave dielectric properties of the fluoride ceramics as a function of sintering temperature. The variations in relative permittivity and quality factor follow the same trend as the relative density for all fluoride ceramics, indicating that relative density is a dominant factor for microwave dielectric properties. The optimum sintering temperature and the best microwave dielectric properties for each composition can be obtained from Fig. 4, and the results are listed in Table 3. Microwave dielectric properties are determined by intrinsic factors and extrinsic factors. Extrinsic factors, such as pores, second phase, and grain boundary [29], can be analysed through the density, XRD, and SEM. Meanwhile, intrinsic factors are closely related to the crystal structure. To reveal the relationship between the microwave dielectric properties of the fluoride ceramics and their crystal structure, some parameters, such as the ionic polarizability of the primitive unit cell, the packing fraction and the bond valence of *A* site (AF_n, *A* = Li, Ca, Sr, Ba; *n* = 1, 2), are calculated based on the Rietveld refinement results.

The influence of porosity on ε_r can be eliminated by the following equation [29]:

$$\varepsilon_r = \varepsilon_{cor}\left(1-\frac{3P(\varepsilon_{cor}-1)}{2\varepsilon_{cor}+1}\right) \qquad (3)$$

ACCEPTED MANUSCRIPT

where ε_{cor} is the relative permittivity of the material corrected for porosity and P is the porosity, which can be calculated by:

$$P = 1 - \rho_{rel} \qquad (4)$$

The relative permittivity of the fluoride ceramics was also calculated by the total ionic polarizability of individual ions (α_D^T) and the mole volume of the primitive unit cell (V_m) according to the Clausius-Mossotti equation [30-32]:

$$\varepsilon_{cal} = \frac{3V_m + 8\pi\alpha_D^T}{3V_m - 4\pi\alpha_D^T} \qquad (5)$$

The total ionic polarizability (α_D^T) of fluorides can be calculated using the following additive rule:

$$\alpha_D^T = \alpha(Li^+) + \alpha(F^-) \quad (6)$$

$$\alpha_D^T = \alpha(A^{2+}) + 2\alpha(F^-) \quad (7)$$

where $\alpha(Li^{2+})$, $\alpha(A^{2+})$, and $\alpha(F^-)$ are the ionic polarizability values of Li^+, A^{2+}, and F^-, respectively, and A represents Ca, Sr and Ba.

Fig. 5 shows the variation in relative permittivity with the ionic polarizability of the primitive unit cell. According to the Clausius-Mossotti equation, the relative permittivity is determined by both V_m and α_D^T. Thus, the ionic polarizability of the primitive unit cell (α_D^T/V_m) is selected as the variable for the X axis. $(\varepsilon_r)_s$ is the dielectric constant of fluoride single crystal reported by Geyer [22]. ε_r, ε_{cor}, ε_{cal} and $(\varepsilon_r)_s$ increase linearly from SrF_2 to LiF with α_D^T/V_m, indicating that the dielectric constant is determined by α_D^T/V_m for different fluoride ceramics. Although the ionic polarizability of Sr^{2+} is larger than that of Ca^{2+}, SrF_2 has a lower dielectric constant than CaF_2. This phenomenon can be attributed to the different V_m values. The ε_{cor}, ε_{cal}

and $(\varepsilon_r)_s$ for each type of fluoride ceramic are very close and higher than experimental dielectric constant ε_r. The lower ε_r than ε_{cal} value for each composition can be attributed to the low relative density (Table 2).

On the basis of the crystal structure information from the Rietveld refinement results, the packing fraction can be calculated by the following equation for AF_n fluoride compounds [33]:

$$\begin{aligned}\text{Packing fraction (\%)} &= \frac{\text{volume of packed ions}}{\text{volume of primitive unit cell}} \\ &= \frac{\text{volume of packed ions}}{\text{volume of unit cell}} \times Z \\ &= \frac{4\pi/3 \times \left(r_A^3 + n r_F^3\right)}{V} \times 4\end{aligned} \quad (8)$$

where r_A and r_F are the effective ionic radii at each coordination number [34], and V is the unit cell volume for fluoride compounds.

As shown in Fig. 6 and Table 3, the quality factors of fluoride single crystal $(Q\times f)_s$ increase with increasing packing fraction, which indicates that the packing fraction plays a dominant role in fluoride single crystal. However, no obvious correlation exists between the packing fraction and the quality factor of fluoride ceramics. For the single crystal, the sample has a slight defect. Thus, $(Q\times f)_s$ is closely related to the intrinsic factor, such as packing fraction. For ceramics, the extrinsic factors, such as pores, grain boundary, and even the raw materials [29], considerably influence the microwave dielectric properties. As shown in Fig. 3(e)-(h), the sintered samples contain many pores, and the grain size distribution is very uneven, which can deteriorate the properties significantly.

Accepted manuscript

ACCEPTED MANUSCRIPT

Bond valence is a useful parameter to explain the relationship between the crystal structure and the microwave dielectric properties, and it has been used to explain the variation of τ_f value in many works [36]. For AF_n fluoride compounds, the bond valence of A site is calculated as follows [33]:

$$V_i = \sum_j v_{ij} \quad (9)$$

$$v_{ij} = \exp\left\{\frac{R_{ij} - d_{ij}}{b}\right\} \quad (10)$$

where R_{ij} is the bond valence parameter, d_{ij} is the bond length between i and j atoms, and b is a constant of 0.37 Å. The bond length d_{ij} is obtained by refinement results.

The τ_f value is related to the coefficient of thermal expansion (α_l) and the temperature coefficient of dielectric constant (τ_ε), and it could be defined as follows [36]:

$$\tau_f = -\alpha_l - \frac{1}{2}\tau_\varepsilon \quad (11)$$

where the variation of τ_f value has an opposite trend to that of with τ_ε value.

The dependence of the τ_f and τ_ε of fluoride ceramics and single crystal on the bond valence of A site (BV_A) is shown in Fig. 7. The τ_f values of fluoride ceramics increase monotonically with the bond valence for A site (BV_A), which means that the bond strength between A and F elements increases monotonically when the A element changes from Li to Ba. Thus, the restoring force and thermal energy increase [33,36], which improves the stability of the structure of the compounds. Therefore, the τ_ε of fluorides decreases as BV_A increases, which is consistent with the results reported by

Accepted manuscript

Geyer et al. Then, the τ_f of the fluoride ceramics in this study rationally moves to the direction of zero on the basis of Eq. (9).

The chemical compatibility between the fluoride ceramics and silver is evaluated. In brief, 20 wt% Ag powders are added to LiF, CaF_2 and BaF_2 ceramics and co-fired at 800 °C, 950 °C and 925 °C for 3 h. Fig. 8 presents the XRD patterns and backscattered electron (BSE) images of the fluoride ceramics. Except for fluoride compounds and Ag, no second phase is observed from the XRD patterns. In Fig. 8(b) and (c), the bright grains are detected as Ag and the dark gray grains as LiF and CaF_2. However, no obvious difference in color contrast exists between the BSE images of BaF_2 and Ag because of their similar molecular weights (Fig. 8(d)). We can only distinguish them from the shape of the grain. In summary, the XRD patterns and BSE prove the good chemical compatibility between LiF, CaF_2 and BaF_2 ceramics and Ag, indicating that LiF, CaF_2 and BaF_2 ceramics are good candidates for LTCC application.

4. Conclusions

The sintering behavior, microstructure and the relationship between the crystal structure and microwave dielectric properties of fluoride ceramics were investigated. LiF, CaF_2, SrF_2 and BaF_2 ceramics could be sintered well at 800 °C, 950 °C, 1050 °C and 925 °C, respectively. All of the sintered samples belong to the Fm-3m (225) space group. For each composition, the relative densities, relative permittivity and quality factor increased monotonously with the sintering temperature before reaching the

maximum value, and the microwave dielectric properties were dominated by the relative densities. For different compositions, the relative permittivity (ε_r), quality factor ($Q\times f$), and temperature coefficient of resonant frequency (τ_f) of the fluoride ceramics linearly increased with the ionic polarizability of the primitive unit cell, packing fraction and bond valence of the *A* site. Among this series of fluoride ceramics, LiF ceramic exhibited the lowest sintering temperature of 800 °C and the highest $Q\times f$ value of 73880 GHz. Given their good chemical compatibility with Ag, LiF, CaF_2, and BaF_2 ceramics are good candidates for LTCC application. This study successfully expanded the research field of microwave dielectric ceramics from oxide ceramics to fluoride ceramics.

Acknowledgments

This work was supported by the National Natural Science Foundation of China (NSFC-51572093 and 51772107). The authors are grateful to the Analytical and Testing Center, Huazhong University of Science and Technology, for SEM analyses.

Reference

[1] X.Y. Du, H. Su, H.W. Zhang, X.T. Liu, X.L. Tang, Phase evolution and microwave dielectric properties of ceramics with nominal composition $Li_{2x}(Zn_{0.95}Co_{0.05})_{2-x}SiO_4$ for LTCC applications, RSC Adv. 7 (2017) 27415-27421.

[2] H.C. Xiang, L. Fang, W.S. Fang, Y. Tang, C.C. Li, A novel low-firing microwave dielectric ceramic $Li_2ZnGe_3O_8$ with cubic spinel structure. J. Eur. Ceram. Soc. 37 (2017) 625-629.

Accepted manuscript

ACCEPTED MANUSCRIPT

[3] H.Z. Zuo, X.L. Tang, H.W. Zhang, Y.M. Lai, Y.L. Jing, H. Su, Low-dielectric-constant $LiAlO_2$ ceramics combined with LBSCA glass for LTCC applications, Ceram. Int. 43 (2017) 8951-8955.

[4] Z.Z. Ding, H. Su, X.L. Tang, H.W. zhang, Y.L. Jing, B.Y. Liu, Low-temperature-sintering characteristic and microwave dielectric properties of $(Zn_{0.7}Mg_{0.3})TiO_3$ ceramics with LBSCA glass, Ceram. Int. 41 (2015) 10133-10136.

[5] H.T. Wu, Q.J. Mei, C.F. Xing, J.X. Bi, Effects of B_2O_3 addition on sintering behavior and microwave dielectric properties of ixiolite-structure $ZnTiNb_2O_8$ ceramics, J. Alloy. Compd. 679 (2016) 26-31.

[6] J. Li, L. Fang, H. Luo, J. Khaliq, Y. Tang, C.C. Li, Li_4WO_5: a temperature stable low-firing microwave dielectric ceramic with rock salt structure, J. Eur. Ceram. Soc. 36 (2016) 243-246.

[7] M. Valant, D. Suvorov, Dielectric properties of the fluorite- like Bi_2O_3-Nb_2O_5 solid solution and the tetragonal Bi_3NbO_7, J. Am. Ceram. Soc. 86 (2003) 939-944.

[8] W. Lei, W.Z. Lu, D. Liu, J.H. Zhu, Phase evolution and microwave dielectric properties of $(1-x)ZnAl_2O_4$-xMg_2TiO_4 ceramics, J. Am. Ceram. Soc. 92 (2008) 105-109.

[9] K.X. Song, X.M. Chen, X.C. Fan, Effects of Mg/Si ratio on microwave dielectric characteristics of forsterite ceramics, J. Am. Ceram. Soc. 90 (2007) 1808-1811.

[10] C.L. Huang, J.Y. Chen, C.C. Liang, Dielectric properties and mixture behavior of $Mg_4Nb_2O_9$-$SrTiO_3$ ceramic system at microwave frequency, J. Alloy. Compd. 78 (2009) 554-558.

[11] D. Klimm, M. Rabe, R. Bertram, R. Uecker, L. Parthier, Phase diagram analysis and crystal growth of solid solutions $Ca_{1-x}Sr_xF_2$, J. Cryst. Growth. 310 (2008) 152-155.

[12] X.Q. Song, K. Du, Z.Y. Zou, Z.H. Chen, W.Z. Lu, S.H. Wang, W. Lei, Temperature-stable $BaAl_2Si_2O_8$-$Ba_5Si_8O_{21}$-based low-permittivity microwave dielectric ceramics for LTCC applications, Ceram. Int. 43 (2017) 14453-14456.

Accepted manuscript

[13] A. Yokoi, H. Ogawa, A. Kan, H. Ohsato, Y. Higashida, Use of LiF to achieve a low-temperature co-fired ceramics (LTCC) with low dielectric loss, J. Ceram. Soc. Jpn. 112 (2004) S1633-S1636.

[14] J. Zhang, Z.X. Yue, Y. Luo, X.H. Zhang, L.T. Li, Novel low-firing forsterite-based microwave dielectric for LTCC applications, J. Am. Ceram. Soc. 99 (2016) 1122-1124.

[15] J.J. Bian, Y. Ding, A new glass-free LTCC microwave ceramic-(1-x)$Li_{2.08}TiO_3$+xLiF, Mater. Res. Bull. 49 (2014) 245-249.

[16] X.H. Zhang, Y.M. Ding, J.J. Bian, Sintering behavior, microstructure and microwave dielectric properties of $Li_2MgTi_3O_8$ modified by LiF, J. Mater. Sci-Mater. El. 28 (2017) 1-6.

[17] J.X. Bi, Y.J. Niu, H.T. Wu, $Li_4Mg_3Ti_2O_9$: a novel low-loss microwave dielectric ceramic for LTCC applications, Ceram. Int. 43 (2017) 7522-7530.

[18] X.H. Wang, H. Jiang, X.C. Wang, Z.L. Li, W.Z. Lu, Microwave dielectric properties of (1-x)MgO-x(0.8LiF-0.2CaF_2) ceramics for low-temperature co-fired ceramics, Ceram. Int. 41 (2015) 12310-12316.

[19] J. Zhang, Z.X. Yue, X.H. Zhang, L.T. Li, Low-temperature sintering and microwave dielectric properties of CaF_2-doped $MgTiO_3$ ceramics, Ceram. Int. 41 (2015) S515-S519.

[20] H.F. Zhou, X.H. Tan, J. Huang, N. Wang, G.C. Fan, X.L. Chen, Phase structure, sintering behavior and adjustable microwave dielectric properties of $Mg_{1-x}Li_{2x}Ti_xO_{1+2x}$ solid solution ceramics, J. Alloy. Compd. 696 (2017) 1255-1259.

[21] M.T. Sebastian, N. Santha, P.V. Bijumon, A.K. Axelsson, N.M. Alford, Microwave dielectric properties of (1-x)CeO_2-$x$$CaTiO_3$ and (1-x)CeO_2-$x$$Sm_2O_3$ ceramics, J. Eur. Ceram. Soc. 24 (2004) 2583-2589.

[22] R.G. Geyer, J. Baker-Jarvis, J. Krupka, Dielectric characterization of single-crystal LiF, CaF_2, MgF_2, BaF_2, and SrF_2 at microwave frequencies, Electrical Insulation and Dielectric Phenomena, 2004, CEIDP'04. 2004 Annual Report Conference on IEEE. 2004;493-497.

Accepted manuscript

ACCEPTED MANUSCRIPT

[23] H.M. Rietveld, A profile refinement method for nuclear and magnetic structures, J. Appl. Cryst. 2 (1969) 65-71.

[24] A.C. Larson, R.B. Dreele, General structure analysis system (GSAS), Los Alamos National Laboratory Report LAUR (1994) 86-748.

[25] B.H. Toby, EXPGUI, a graphical user interface for GSAS, J. Appl. Cryst. 34 (2001) 210-213.

[26] B.W. Hakki, P.D. Coleman, A dielectric resonator method of measuring inductive capacities in the millimeter range, IRE. Trans. Microwave Theory Technol. 8 (1960) 402-410.

[27] S.H. Lei, H.Q. Fan, W.N. Chen, Z.Y. Liu, M.M. Li, Structure, microwave dielectric properties, and novel low- temperature sintering of xSrTiO$_3$-(1-x)LaAlO$_3$ ceramics with LTCC application, J. Am. Ceram. Soc. 100 (2017) 235-246.

[28] J.W. Bullard, A.W. Searcy, Microstructural development during sintering of lithium fluoride, J. Am. Ceram. Soc. 80 (1997) 2395-2400.

[29] J.X. Bi, C.F. Xing, C.H. Yang, H.T. W, Phase composition, microstructure and microwave dielectric properties of rock salt structured Li_2ZrO_3-MgO ceramics, J. Eur. Ceram. Soc. 38 (2018) 3840-3846.

[30] L.X. Pang, D. Zhou, W.B. Li, Z.X. Yue, High quality microwave dielectric ceramic sintered at extreme-low temperature below 200^o and co-firing with base metal, J. Eur. Ceram. Soc. 37 (2017) 3073-3077.

[31] L.X. Pang, D. Zhou, Z.M. Qi, Z.X. Yue, Influence of W substitution on crystal structure, phase evolution and microwave dielectric properties of ($Na_{0.5}Bi_{0.5}$)MoO_4 ceramics with low sintering temperature. Sci. Rep. 7 (2017) 3201.

[32] R.D. Shannon, Dielectric polarizabilities of ions in oxides and fluorides, J. Appl. Phys. 73 (1993) 348-366.

[33] E.S. Kim, B.S. Chun, R. Freer, R.J. Cernik, Effects of packing fraction and bond valence on microwave dielectric properties of $A^{2+}B^{6+}O_4$ (A^{2+}: Ca, Pb, Ba; B^{6+}: Mo, W) ceramics, J. Eur. Ceram. Soc. 30 (2010) 1731-1736.

[34] R.D. Shannon, Revised effective ionic radii and systematic studies of interatomic distances in halides and chalcogenides, Acta crystallogr. A. 32 (1976) 751-767.

[35] D. Zhou, H. Wang, L.X. Pang, C.A. Randall, X. Yao, Bi_2O_3-MoO_3 binary system: an alternative ultralow sintering temperature microwave dielectric, J. Am. Ceram. Soc. 92 (2009) 2242-2246.

[36] M.K. Du, L.X. Li, S.H. Yu, Z. Sun, J.L. Qiao, High-Q microwave ceramics of Li_2TiO_3 co-doped with magnesium and niobium, J. Am. Ceram. Soc. 101 (2018) 4066-4075.

Table Caption:

Table 1 Sintering temperatures and microwave dielectric properties of some microwave dielectric ceramics doped with different fluorides

Composition	Sintering aid	T_s (°C)	ε_r	$Q\times f$ (GHz)	τ_f (ppm/°C)	Ref.
$BaAl_2Si_2O_8$	LiF	900	6.81	47030	-25.4	[12]
$Mg_4Nb_2O_9$	LiF	850	12.60	103607	-70.5	[13]
Mg_2SiO_4	LiF	800	6.81	167000	-47.9	[14]
$Li_{2.08}TiO_3$	LiF	900	22.80	63000	+1.0	[15]
$Li_2MgTi_3O_8$	LiF	850	27.80	63000	-4.1	[16]
$Li_4Mg_3Ti_2O_9$	LiF	900	15.17	42800	-11.3	[17]
MgO	$0.8LiF\text{-}0.2CaF_2$	950	9.18	130198	-65.0	[18]
$MgTiO_3$	CaF_2	1050	17.51	37000	+4.8	[19]

T_s: Sintering temperature

Table 2 The lattice parameters and density of fluoride ceramics sintered at their densification temperatures

Composition	$a = b = c$ (Å)	V (Å^3)	Z	V_m (Å^3)	ρ_{bul} (g/cm^3)	ρ_{the} (g/cm^3)	ρ_{rel} (%)	Rwp	Rp	χ^2
LiF	4.027	65.308	4	16.327	2.381	2.638	90.273	7.62	5.52	4.969
CaF_2	5.464	163.085	4	40.771	2.987	3.180	93.943	12.58	10.53	2.927
SrF_2	5.803	195.398	4	48.850	3.907	4.270	91.508	10.62	8.36	5.627
BaF_2	6.202	238.533	4	59.633	4.493	4.882	92.041	11.94	9.65	4.550

Table 3 Packing fraction (PK), bond valence of *A* site (BV_A) and microwave dielectric properties of fluoride ceramics and single crystal

Composition	T_s (°C)	ε_r	ε_{cor}	ε_{cal}	$(\varepsilon_r)_s$	$Q\times f$ (GHz)	$(Q\times f)_s$ (GHz)	PK (%)	τ_f (ppm/°C)	$(\tau_\varepsilon)_s$ (ppm/°C)	BV_A
LiF	800	8.02	9.15	8.85	9.00	73880	192400	71.6	-117.7	+257	1.026
CaF_2	950	6.48	6.99	6.76	6.78	26448	92000	60.6	-95.69	+238	1.942
SrF_2	1050	5.85	6.5	6.37	6.48	51132	73000	55.7	-80.20	+230	2.101
BaF_2	925	6.72	7.44	7.29	7.35	53654	57600	51.7	-74.20	+204	2.203

Note: microwave dielectric properties of single crystal reported in Ref. [22] are remarked by subscript "( )$_s$". T_s: sintering temperature.

Figure Caption:

Fig. 1 XRD patterns of fluoride raw materials: (a) LiF; (b) CaF_2; (c) SrF_2; (d) BaF_2; and the sintered fluoride ceramics: (e) LiF, 800 °C; (f) CaF_2, 950 °C; (g) SrF_2, 1050 °C; (h) BaF_2, 925°C

Fig. 2 The results of Rietveld refinement for fluoride ceramics: (a) LiF, 800 °C; (b) CaF_2, 950 °C; (c) SrF_2, 1050 °C; (d) BaF_2, 925°C

Fig. 3 SEM images of the sintered fluoride ceramics: (a) LiF, 800 °C; (b) CaF_2, 950 °C; (c) SrF_2, 1050 °C; (d) BaF_2, 925°C； and (e) mechanism of grain growth

Fig. 4 The variation in relative densities, ε_r and $Q\times f$ of fluoride ceramics with sintering temperature: (a) LiF; (b) CaF_2; (c) SrF_2; (d) BaF_2

Fig. 5 The variation in dielectric constant with the ionic polarizability of primitive unit cell

Fig. 6 The variation in quality factor of fluoride ceramics and single crystal with the packing fraction

Accepted manuscript

ACCEPTED MANUSCRIPT

Fig. 7 The variation in τ_f and τ_ε of fluoride ceramics and single crystal with the bond valence of *A* site

Fig. 8 (a) XRD patterns of fluoride ceramics co-fired with 20 wt% Ag powders; and BSE images of fracture surface: (b) LiF-20 wt% Ag, 800 °C; (c) CaF_2-20 wt% Ag, 950 °C; (b) BaF_2-20 wt% Ag, 925 °C

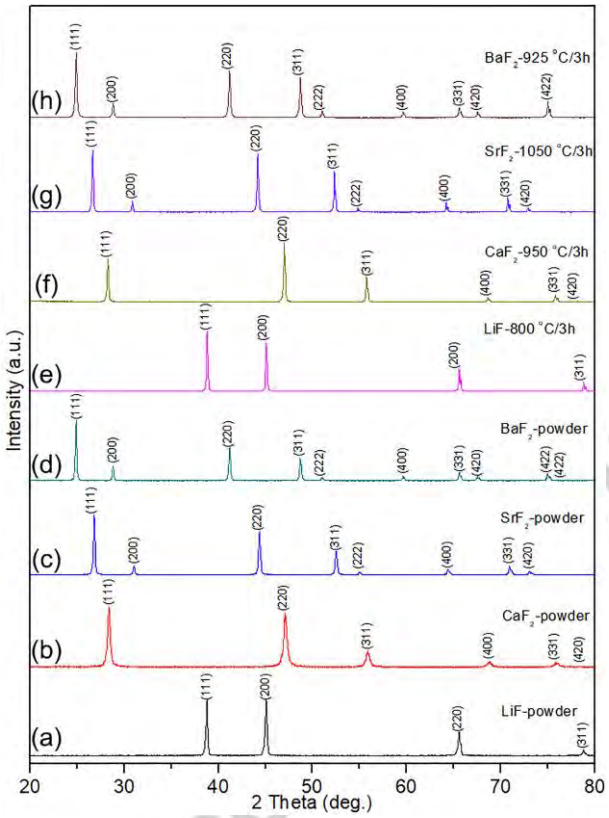

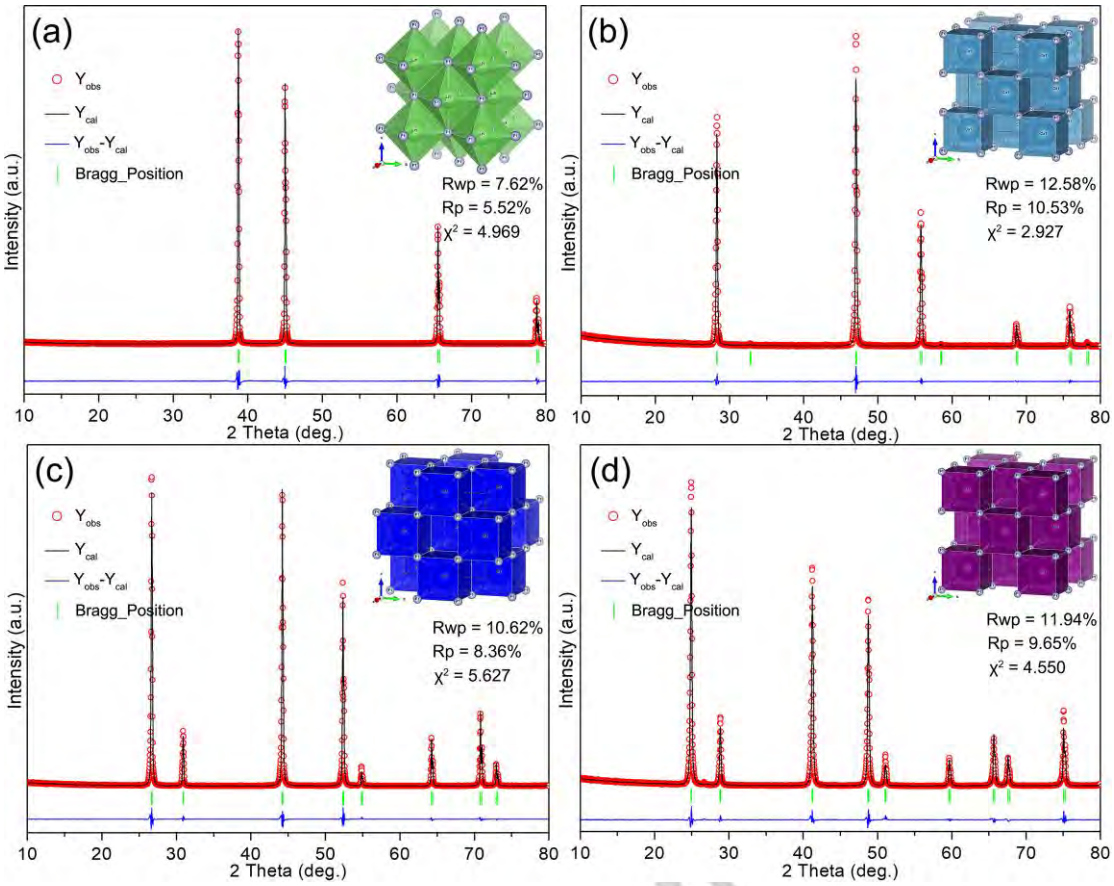
(a)
Y_obs
Y_cal
Y_obs-Y_cal
Bragg_Position
Rwp = 7.62%
Rp = 5.52%
χ² = 4.969
Intensity (a.u.)
2 Theta (deg.)
(b)
Rwp = 12.58%
Rp = 10.53%
χ² = 2.927
(c)
Rwp = 10.62%
Rp = 8.36%
χ² = 5.627
(d)
Rwp = 11.94%
Rp = 9.65%
χ² = 4.550

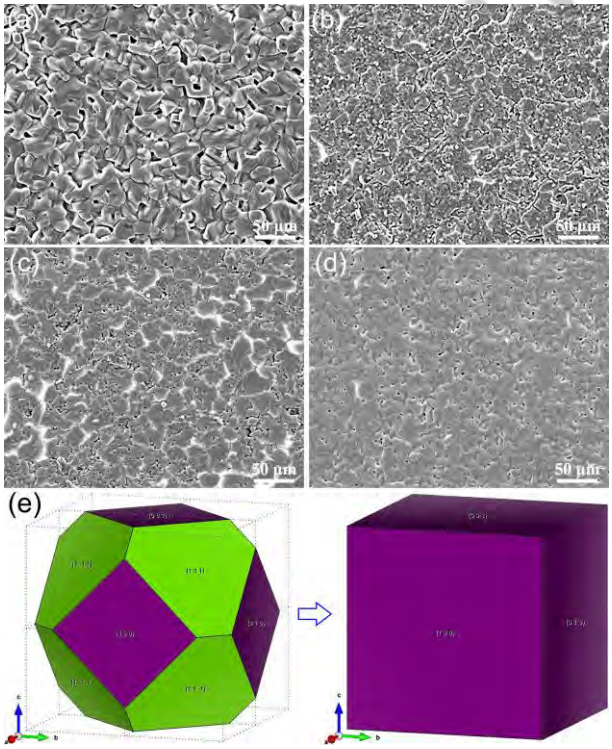
(a)
(b)
(c)
(d)
(e)

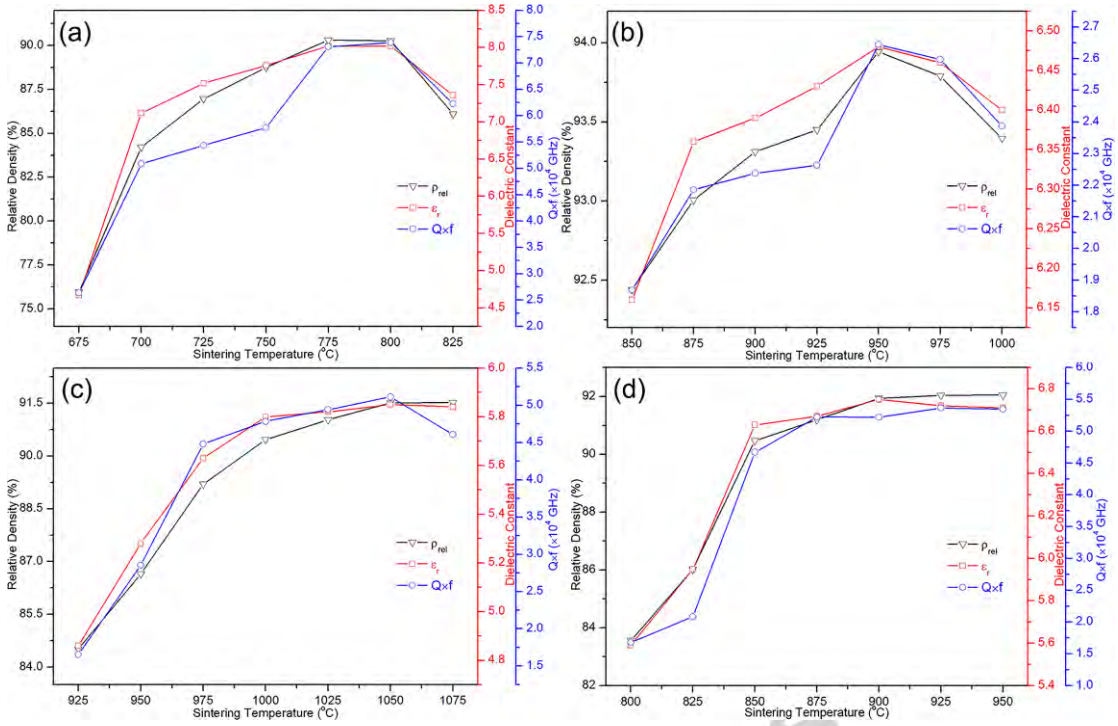
(a)
(b)
(c)
(d)
Relative Density (%)
Dielectric Constant
Q×f (×10⁴ GHz)
Sintering Temperature (°C)
ρrel
εr
Q×f

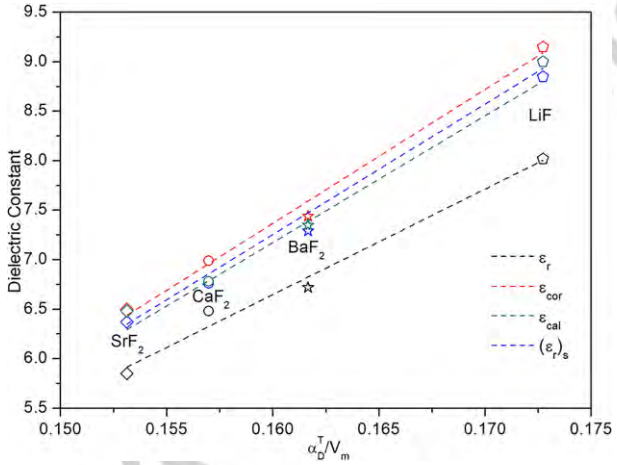
Dielectric Constant
LiF
BaF2
CaF2
SrF2
εr
εcor
εcal
(εr)s
αDT/Vm

ACCEPTED MANUSCRIPT